NATIONAL ADVISORY COMMITTEE FOR AERONAUTICS

TECHNICAL MEMORANDUM 1285

INVESTIGATIONS OF THE WALL-SHEARING STRESS IN TURBULENT BOUNDARY LAYERS

By H. Ludwieg and W. Tillmann

Translation of "Untersuchungen über die Wandschubspannung in turbulenten Reibungsschichten"

NACA

Washington

May 1950

NATIONAL ADVISORY COMMITTEE FOR AERONAUTICS

TECHNICAL MEMORANDUM 1285

INVESTIGATIONS OF THE WALL-SHEARING STRESS IN TURBULENT BOUNDARY LAYERS*

By H. Ludwieg and W. Tillmann

SUMMARY

Because of the unsatisfactory state of knowledge concerning the surface shearing stress of boundary layers with pressure gradients, the problem is re-examined. It is found that for general turbulent boundary layers in wall proximity, that is, in the laminar sublayer, in the transition zone and in the part of the completely turbulent zone near the wall, the same universal law applies as for the plate flow. From the general validity of this law a formula was deduced for the local drag coefficient c_f', in which c_f' depends only on the Reynolds number Re formed with the momentum thickness and on a profile parameter γ. This relation was confirmed satisfactorily by direct measurements with a new instrument. The related friction coefficient c_f' can then be determined simply from the known velocity profile.

From the formula for c_f' it follows, in agreement with the tests, that the c_f' values for boundary layers with accelerating and decelerating pressure are higher and lower, respectively, than for the plate flow at equal Reynolds number. Thus for greater Reynolds numbers small local drag coefficients are attainable not only by keeping the boundary layer laminar but also by appropriate pressure variation in turbulent boundary layers. The rise of the friction coefficient to a multiple of that for plate flow in boundary layers with pressure rise, as claimed by various workers, is herewith disproved.

I. INTRODUCTION

The wall-shearing stresses in laminar boundary layers can be computed on a strictly theoretical basis, since the relationship between velocity profile and shearing stress is known. But, this procedure can not be applied to the turbulent boundary layers since the relationship

*"Untersuchungen über die Wandschubspannung in turbulenten Reibungsschichten."

for the shearing stresses due to the turbulent exchange is still unknown. For this reason, the laws for turbulent wall friction must be determined by experimental investigations. Such investigations fall into two classes, termed for brevity, "plate flows" and "pipe and channel flows." The approximate formulas for the friction drag, deduced by the various investigators from the test data, are in agreement to some extent.

Some investigations have been made also on boundary layers with pressure gradients, both accelerating and decelerating, but the data on wall friction are either absent altogether or partly unsatisfactory. These investigations were made in a channel of circular section (reference 1) or, in most cases, of rectangular section (references 2, 3, 4, and 5). For the latter, one channel wall was designed as flat test plate, on which the boundary layer to be explored was measured. The opposite wall was adjustable to the desired pressure distribution. It was spaced far enough from the experimental surface to maintain a core with potential flow between the two boundary layers (free boundary layer). The wall-shearing stress was determined from the measured velocity profile by means of von Kármán's momentum equation. The advantage of this method rests in the fact that thick boundary layers (high Reynolds numbers) can be produced with a comparatively small layout. One substantial drawback is the narrow width of the experimental flow compared to the boundary-layer thickness. This is likely to produce secondary flows which cancel the two-dimensionality of the flow assumed according to von Kármán's momentum equation for the interpretation, and are presumably responsible for the improbable results of the aforementioned authors. Some of these authors had observed that, in greatly retarded flows, the local drag coefficient c_f' ($= \tau_w/Q$, τ_w = wall-shearing stress, Q the dynamic pressure outside the boundary layer) rose abruptly to a multiple of its original value after traveling a certain distance in flow direction, rather than decreased, as actually anticipated analogous to the behavior of the laminar flow. Since no valid reason could be found for it, Tillmann (reference 6) made an investigation in an attempt to find out whether this effect was simulated by secondary flows. The velocity in a section across the tunnel was measured in magnitude and direction. An appraisal of the effect of the observed secondary flows gave a c_f' value lower by 40 percent. This fact made the test method employed up to then questionable.

Quite recently, Ludwieg (reference 7) developed a simple instrument by means of which the wall-shearing stress can be determined at any test station by a heat-transfer measurement. This direct method is not affected by any secondary flows. The investigation of the frictional drag of turbulent boundary layers with pressure gradients, both accelerating and decelerating, repeated with this new instrument, forms the subject of the present report.

II. THEORETICAL CONSIDERATIONS ON FRICTIONAL DRAG

The results of previous investigations of plate and pipe flows were as follows:

(a) The velocity profile of the boundary layer can be represented in the form

$$\frac{u}{U} = g\left(\frac{y}{\delta_2}, \text{Re}\right) \qquad (1)^1$$

(u = velocity in boundary layer, U = velocity outside boundary layer, y = wall distance); $\delta_2 = \int_0^\infty \frac{u}{U}\left(1 - \frac{u}{U}\right)dy$ = momentum thickness of boundary layer, $\text{Re} = U\frac{\delta_2}{\nu}$ = Reynolds number of boundary layer formed with momentum thickness δ_2; ν = kinematic viscosity.

Quantity g in equation (1) is a fixed function which, however, is, naturally, different for plate, pipe, and channel flow. The dependence of $\frac{u}{U}$ on Re is very small, that is, the velocity profiles differ very little for different Reynolds numbers.

(b) The local friction coefficient c_f' can always be represented in the form

$$c_f' = F(\text{Re}) \qquad (2)$$

($c_f' = \tau_w/\frac{\rho}{2}U^2$; τ_w = wall-shearing stress; ρ = density).

Quantity F is again a fixed function for plate, pipe, and channel flow; F can be computed for plate flow by the momentum equation when g is known, because the total friction drag appears as loss of momentum in the boundary layer.

(c) For the part of the velocity profiles near the wall, the relation

$$\frac{u}{u^*} = f\left(\frac{u^* y}{\nu}\right) \qquad (3)$$

was obtained. ($u^* = \sqrt{\tau_w/\rho}$ = shearing stress velocity)

---

[1] In this formula, the Reynolds number formed with the momentum thickness δ_2 was chosen as characteristic quantity because it is more appropriate for boundary layers with variable outside pressure.

This relation holds true with the same function f for the part of plate, pipe, or channel flow next to the wall. Provided that the $\frac{u^*y}{\nu}$ values are not too small $\left(\text{fully turbulent zone } \frac{u^*y}{\nu} > 50\right)$, equation (3) can be replaced very accurately by the approximate formula

$$\frac{u}{u^*} = a \log \frac{u^*y}{\nu} + b \tag{3a}$$

a and b being universal constants. This logarithmic law can be approximated by a power law

$$\frac{u}{u^*} = C\left(\frac{u^*y}{\nu}\right)^{1/n} \tag{3b}$$

where C and n are constants which are still somewhat dependent on the u^*y/ν zone for which the approximation is to be especially good.

As already stated in Ludwieg's report (reference 7), it is to be expected that the universal law, equation (3) or (3a), is, aside from the plate, pipe, and channel flow, applicable also to more generalized boundary-layer flows in wall proximity. It even should hold for velocity profiles diverging considerably from the profiles in plate flow and for flows with marked pressure gradients.

A definite experimental proof of the general validity of the law, equations (3) and (3a), is afforded from the fact originally established by Wieghardt (reference 8); namely, that when the boundary-layer profiles are plotted in the manner of $\log u/U$ against $\log y/\delta_2$ (fig. 1), parallel straight lines are obtained for small y/δ_2. Consequently, u is in all cases proportional to the same power of y. From the slope of the straight lines, this power follows as $0.13 = \frac{1}{7.7}$, which is in good agreement with equation (3b) for the u^*y/ν range in question. However, this still is no compelling proof of the validity of equation (3b) for the reason that the power of y can be checked by profile measurement, but not the constant C, because u^* is unknown.

With the validity of equation (3) for the portion of the boundary layer next to the wall, u^* and, hence, τ_w and c_f' depend only on the velocity profile and the material constants of the flowing medium; so, when the velocity profile is known, c_f' can be computed. A corresponding relation between c_f', Re, and a profile parameter yet to be defined is derived in the following.

The term $\gamma = \frac{u_{\delta_2}}{U}$ is introduced as profile parameter; u_{δ_2} is defined as follows: If the law, equations (3), (3a), and (3b), is valid for y values greater than δ_2, then u_{δ_2} is simply the value of u at the point $y = \delta_2$. But, if the law, equations (3), (3a), and (3b), applies only to y values smaller than δ_2, then u_{δ_2} is the value which u would assume if the law, equations (3), (3a), and (3b), were applicable up to the point $y = \delta_2$.[2] Thus, the double logarithmic plotting of u/U against y/δ_2 (fig. 1) gives the profile parameter γ, when the rectilinear part of the profile is extended as far as $\frac{y}{\delta_2} = 1$, and the corresponding value of $\frac{u_{\delta_2}}{U}$ is read from figure 1.

The derivation of the above-mentioned relation between c_f', Re, and γ proceeds from equation (3). The profile parameter is introduced by putting $y = \delta_2$ and $u = u_{\delta_2}$. Then,

$$\frac{u_{\delta_2}}{u^*} = f\left(\frac{u^*\delta_2}{\nu}\right) = f\left(\frac{u_{\delta_2}\delta_2}{\nu}\ \frac{u^*}{u_{\delta_2}}\right) \tag{4}$$

The equation states that a direct connection exists between u^*/u_{δ_2} and $u_{\delta_2}\delta_2/\nu$; therefore

$$\frac{u^*}{u_{\delta_2}} = h\left(\frac{u_{\delta_2}\delta_2}{\nu}\right)$$

must be applicable, the function h being defined by function f.

Introduction of

$$u^* = \sqrt{\frac{\tau_w}{\rho}} = U\sqrt{\frac{c_f'}{2}}\ ,\ \frac{u_{\delta_2}}{U} = \gamma,\ \text{and}\ \frac{U\delta_2}{\nu} = \text{Re}$$

---

[2] Gruschwitz (reference 2) defined the quantity $\eta = 1 - \left(\frac{u_{\delta_2}}{U}\right)^2$ as profile parameter; but by u_{δ_2} the value of u at $y = \delta_2$ is always meant.

gives, after simple rearrangement

$$c_f' = 2\gamma^2 h^2(\mathrm{Re}\ \gamma) = \gamma^2 H(\mathrm{Re}\ \gamma) \tag{5}$$

For abbreviation, the function is written $2h^2 = H$.

So, for all turbulent boundary-layer profiles whose part next to the wall is represented by the general law, equation (3), the friction coefficient is given in the form of equation (5). To define the functions h and H in this equation, equation (4) could be replaced, for the argument in question in accordance with equation (3a), by

$$\frac{u_{\delta_2}}{u^*} = a \log \frac{u^* \delta_2}{\nu} + b = a \log \left(\frac{u_{\delta_2} \delta_2}{\nu} \frac{u^*}{u_{\delta_2}} \right) + b$$

and numerically solved for $\frac{u^*}{u_{\delta_2}} = h$. But since the constants a and b in equation (3a) are not accurately enough known, the following method of defining H seems to be more appropriate.

By equation (1), the profile parameter for the profiles of the plate flow, designated γ_0, is only dependent on Re, hence $\gamma_0 = \gamma_0(\mathrm{Re})$. On inserting this value in equation (5), this equation must supply the drag coefficient c_f' for the plate flow. Thus, bearing in mind equation (2), the functional equation for H follows as

$$\gamma_0^2 H(\mathrm{Re}\ \gamma_0) = F(\mathrm{Re}) \tag{6}$$

where F(Re) is the friction coefficient of the plate flow. This equation, which must be fulfilled for all Re, definitely defines the function H for known functions F(Re) and $\gamma_0(\mathrm{Re})$.

Abbreviating

$$\mathrm{Re}\ \gamma_0(\mathrm{Re}) = \xi$$

iteration gives for Re the chain function

$$\mathrm{Re} = \frac{\xi}{\gamma_0\left(\frac{\xi}{\gamma_0\left(\frac{\xi}{\gamma_0\left(\cdots\right)}\right)}\right)}$$

which, inserted in equation (6) gives for H

$$H(\xi) = \frac{1}{\gamma_0^2\left(\frac{\xi}{\gamma_0\left(\frac{\xi}{\gamma_0\left(---\right)}\right)}\right)} F\left(\frac{\xi}{\gamma_0\left(\frac{\xi}{\gamma_0\left(\frac{\xi}{\gamma_0\left(---\right)}\right)}\right)}\right)$$

and, when the function H in equation (5) is then replaced by the preceding expression,

$$c_f' = \frac{\gamma^2}{\gamma_0^2\left(\mathrm{Re}\,\frac{\gamma}{\gamma_0\left(\mathrm{Re}\,\frac{\gamma}{\gamma_0\left(---\right)}\right)}\right)} F\left(\mathrm{Re}\,\frac{\gamma}{\gamma_0\left(\mathrm{Re}\,\frac{\gamma}{\gamma_0\left(---\right)}\right)}\right) \tag{7}$$

Since γ_0 varies very little with Re (fig. 2), the convergence of the chain function is so good that in the first factor only the term of the first degree and in the second factor, the term of zero degree have to be included. Therefore

$$c_f' = \frac{\gamma^2}{\gamma_0^2\left(\mathrm{Re}\,\frac{\gamma}{\gamma_0(\mathrm{Re})}\right)} F\left(\mathrm{Re}\,\frac{\gamma}{\gamma_0(\mathrm{Re})}\right) \tag{8}$$

This formula gives the friction coefficient c_f' for general boundary layers (for example, with pressure rise or fall) in relation to the Reynolds number Re and the profile parameter γ. It was derived on the assumption that the universal law, equation (3), is applicable in wall proximity. The functions F and γ_0 can be taken from the experimental data on plate flow.

As an approximation, it is sufficient to insert in equation (8) the functions F and γ_0 which follow from the assumption of the conventional 1/7 power law for the velocity profile. Owing to the affinity of the profiles, γ_0 is unaffected by Re and can be computed by a simple integration which gives the value $\gamma_0 = 0.717$. The corresponding function F with Gruschwitz's numerical constant (reference 2) reads

$$c_f' = F(\mathrm{Re}) = 0.0251\ \mathrm{Re}^{-1/4}$$

From these values for γ_0 and F, inserted in equation (8), follows

$$c_f' = 0.0449\gamma^{7/4}Re^{-1/4}$$

Since the 1/7 power law for the velocity distribution and the subsequent 1/4 power law for the friction coefficient are valid only in rough approximation, the derived c_f' formula is comparatively inaccurate. A better adaptation to the actually appearing drag coefficients is obtained by a slight change in the numerical constants, which results in the formula

$$c_f' = 0.0580\gamma^{1.705}Re^{-0.268} \qquad (9)$$

This formula approximates equation (8) quite closely, when the function F is replaced by the Schultz-Grunow plate friction law (explained in the next section) and the function γ_0 by the curve represented in figure 2. In the range of $1 \times 10^3 \leq Re \leq 4 \times 10^4$, the discrepancies are less than 3 percent.

From the simple approximate formula (9), it is seen that at constant Re the drag coefficient c_f' is proportional to $\gamma^{1.705}$. Since γ decreases along the test length for boundary layers with pressure rise and Re increases, c_f' decreases sharply, which is entirely contrary to the findings of Mangler (reference 4) and Wieghardt (reference 5), who identified a substantial increase of the c_f' value; therefore, it was decided to check the relation (8) derived for the friction coefficient c_f' by experiments which will be described in the following.

III. BEHAVIOR OF DRAG COEFFICIENT IN BOUNDARY LAYERS WITH PRESSURE GRADIENTS

The boundary layers were investigated in the same test length of rectangular cross section, as already described by Schultz-Grunow (reference 9) and which had been designed according to the conventional principle for boundary-layer measurements explained in the introduction of the present report. But, while their adjustable wall had been set for constant pressure over the test length, the wall, in the present study, was adjusted so that the desired pressure variation resulted. The velocity profiles of the boundary layers were determined at ten to

twelve stations along the center line of the smooth, flat plate (1.4 × 6m). The wall shearing stress was measured at the same points by means of Ludwieg's instrument (reference 7).

Altogether, four different test series were carried through:

(a) At constant pressure in flow direction (plate flow)

(b) At moderate pressure rise

(c) At strong pressure rise

(d) At pressure drop

The instrument was calibrated prior to the measurements and in the following manner: The channel was set for plate flow and the instrument mounted at two different stations on the plate. Each test run covered the entire speed range, the corresponding calibration shearing stress being determined by the friction law for plate flow. From the available approximation formulas for the drag coefficient of plate flow, the Schultz-Grunow formula (reference 9)

$$^{3}\ c_{f'} = \frac{0.0334}{(\log \mathrm{Re})^{1.838}}$$

was used, since it was obtained on measurements in the same experimental setup. As a check, the wall-shearing stress was measured with the calibrated instrument along the entire test length at constant speed. The function $\gamma_0 = \gamma_0(\mathrm{Re})$ used for checking equation (8) was determined from the simultaneously measured velocity profiles. It is plotted against $\log \mathrm{Re}$ in figure 2, along with the γ_0 from the Schultz-Grunow measurements, for comparison. The writer's test points lie somewhat above the Schultz-Grunow curve at small Re numbers. The heavy solid curve is used as basis in the subsequent interpretations.

In figure (3a), the drag coefficient $c_{f'}$ is plotted double logarithmically against the Re number for the four test series, along with the Schultz-Grunow friction law for comparison. The test points of the series made as a check at constant pressure (plate flow) coincide with the Schultz-Grunow curve and, thus, prove the correctness of the

---

[3] In the Schultz-Grunow report, $c_{f'}$ is indicated as function of the Reynolds number formed with length x; in the present article, it is reduced to the Reynolds number Re formed with the momentum thickness δ_2.

calibration measurement. The two test series with moderate and strong pressure rise exhibit c_f' values at the end of the test length, which are considerably below the Schultz-Grunow curve for plate flow. This therefore means that the assumption of a c_f' value depending on Re only, as used by Buri (reference 1), Gruschwitz (reference 2), Squire and Young (reference 10), Kehl (reference 3), and von Doenhoff and Tetervin (reference 11) as basis for computing turbulent boundary layers with pressure gradients, is not correct. It refutes, in particular, the test data of Mangler (reference 4) and Wieghardt (reference 5), who claimed a marked increase in c_f' on boundary layers in retarded flow after a certain entrance length in flow direction. The test points of the series, with pressure drop, are located a little above the Schultz-Grunow curve.

Following these preparations, we proceed to the checking of equation (8). To simplify the mode of writing of this equation, the following abbreviation is introduced:

$$\gamma_0\left(\mathrm{Re}\,\frac{\gamma}{\gamma_{0(\mathrm{Re})}}\right)=\tilde{\gamma}_0$$

After putting equation (8) in the following form

$$c_f'\left(\frac{\tilde{\gamma}_0}{\gamma}\right)^2 = F\left(\mathrm{Re}\,\frac{\gamma}{\gamma_{0(\mathrm{Re})}}\right) \qquad (8a)$$

the same functional relationship existing between Re and c_f' in plate flow prevails also between $c_f'\left(\frac{\tilde{\gamma}_0}{\gamma}\right)^2$ and $\mathrm{Re}\,\frac{\gamma}{\gamma_{0(\mathrm{Re})}}$. Thus figure (3b) shows $\log\left[c_f'\left(\frac{\tilde{\gamma}_0}{\gamma}\right)^2\right]$ plotted against $\log\left(\mathrm{Re}\,\frac{\gamma}{\gamma_0}\right)$ along with the Schultz-Grunow law for plate flow. If equation (8) is correct, the points of all test series must fall on the plotted curve. The points of the test series with constant pressure were simply transferred from figure (3a), since a recalculation is superfluous. The points of the remaining test series lie satisfactorily on the Schultz-Grunow curve. The test points of the series with pressure rise, which result in considerably smaller c_f' values than the corresponding plate flow, are in especially good agreement with the Schultz-Grunow curve, and so prove equation (8) in

the best conceivable manner. Only the recomputed points of the series with pressure drop lie a little below the plotted curve, but this does not imply a failure of equation (8) because the Schultz-Grunow law is rather uncertain at small Re numbers, as seen from a comparison with the approximate formulas of other authors (references 10, 12, 13, 14, and 15), which depart from the Schultz-Grunow curve by the same order of magnitude as the present test points.

From equation (8) (or even more readily apparent according to the approximate equation (9)), it follows that with approach to the point of separation of a turbulent boundary layer ($\gamma \rightarrow 0$), the drag coefficient c_f' tends toward zero. So, close to the zone of separation, very small c_f' values must appear, which we have attempted to prove in the test series with strong pressure rise. It resulted in a c_f' value of 0.0010 instead of a c_f' of 0.0020 for plate flow at the same Re number. No acceptable lower drag coefficients could be obtained with the experimental setup because the flow separated first in the corners of the tunnel section.

For the derivation of equation (8), it was assumed that the universal law, equation (3) for the wall-adjacent part of the velocity profiles in the boundary layer is applicable also to general boundary layers. Therefore, all profiles in the representation of u/u^* against $\log \frac{u^* y}{\nu}$ must coincide in wall proximity. This behavior is satisfactorily confirmed on several profiles chosen at random represented in figure 4. The shearing stress velocities u^* were determined from the thermally measured c_f' values. In this semilogarithmic representation the coincident wall-adjacent profile portion is a straight line, by reason of equation (3a). Only the test points nearest to the wall lie a little below this straight line, since they are no longer in the completely turbulent range of the velocity profile, but in the transitional zone to the laminar sublayer (Reichardt's measurements, reference 16). In this representation, the profile shape with pressure rise or drop is affected only in the part away from the wall.

IV. SINGLE PARAMETRIC CHARACTERISTIC OF TURBULENT BOUNDARY-LAYER PROFILES

The single parametric characteristic of turbulent velocity profiles at any pressure variation, found by Gruschwitz (reference 2) and reproduced in figure 1, has been consistently verified by various authors (references 3, 8, and 11), but has not been explained. The reason for

the approximately single parametric characteristic is apparent from the data of the foregoing.

As seen in figure 4, all boundary-layer profiles near the wall coincide in the representation of u/u^* against u^*y/ν $\left(\text{or } \log \frac{u^*y}{\nu}\right)$. From it, the representation u/U against y/δ_2 in which, according to Gruschwitz, all profiles are to form a one-parameter family of curves, are obtained by affine distortion of the ordinate with u^*/U and the abscissa with $\nu/u^*\delta_2$. Since both quantities u^*/U and $\nu/u^*\delta_2$ are independent of one another, it might be expected that even the wall-adjacent part of the velocity profile would become two-parametric in the representation u/U against y/δ_2. But the general velocity law, equation (3), which applies to the coincident wall-adjacent part of the profile in figure 4, can be approximated by a simple power law, (3b), outside of the laminar sublayer. A power law with any mutually unaffected affine distortions in ordinate and abscissa direction always changes again into power laws with the same exponent, which give a single-parametric family of profiles in wall proximity.

The adjoining part of the velocity profile, in which the velocity varies very slowly, is amply defined for given wall-adjacent part. Since the joining must take place continuously and with continuous derivatives, the profile must approach the value $\frac{u}{U} = 1$ asymptotically, and the integral must be $\int_0^\infty \frac{u}{U}\left(1 - \frac{u}{U}\right)d\left(\frac{y}{\delta_2}\right) = 1$ (definition of momentum thickness).

However, this single-parametric characteristic for the velocity profile refers only to the turbulent part of the profile and does not include the laminar sublayer.

Since, by reason of the single-parametric characteristic, the velocity profiles can be definitely identified by any parameter, the connection between two profile parameters must be definite. This is represented in figure 5 for γ and quantity H_{12}, H_{12} being the ratio of displacement thickness[4] δ_1 to momentum thickness δ_2. In this plot, the test points which correspond to dissimilar profiles from all test series lie very nicely on one curve (with exception of the test series "constant pressure and strip"; see next section), which confirms the single-parametric characteristic in the best conceivable manner.

---

[4] Displacement thickness $\delta_1 = \int_0^\infty \left(1 - \frac{u}{U}\right)dy$.

Consequently, H_{12} is a suitable profile parameter, because this quantity is used frequently in computations of the turbulent boundary layers, and it is natural to use it in equation (9) instead of γ. The relationship between γ and H_{12}, represented in figure 5, can be approximated by the formula

$$\gamma = 2.333 \times 10^{-0.398 H_{12}}$$

which, introduced in equation (9), gives the approximate formula

$$c_f' = 0.246 \times 10^{-0.678 H_{12}} \times Re^{-0.268} \qquad (9a)$$

which reproduces the drag coefficients c_f' in relation to profile parameter H_{12} and Reynolds number Re satisfactorily.

V. SCOPE OF APPLICATION OF THE ESTABLISHED CORRELATIONS

After the results obtained in the foregoing have proved true for boundary layers with pressure gradients, the next problem is to check the extent of validity of the derived relations at any disturbance of the boundary layer. Two additional series of tests were made, namely,

(e) At constant pressure and with turbulence grid

(f) At constant pressure and with square strip

For the measurements of the first test series, a setup described by Wieghardt (reference 17) was used. A coarse screen of metal strips was placed before the tunnel nozzle which increased the turbulence of the air flow considerably (diminution of the critical sphere characteristic coefficient UD/ν from 3.75×10^5 to 1.3×10^5). The rest of the procedure was the same as for the test series at constant pressure (a). In figure 6a, the measured c_f' is plotted against the Reynolds number Re in double logarithmic representation. The increased turbulence of the outer flow has increased the friction coefficient on an average of 10 percent compared to the plate flow. In figure 6b, $c_f'\left(\frac{\tilde{\gamma}_0}{\gamma}\right)^2$ is plotted again against $\left(Re\,\frac{\gamma}{\gamma_0}\right)$ in double logarithmic representation, corresponding to figure 3b. The test points of this series coincide with the test points for the plate flow, thus proving the applicability of equation (8) to such intensely turbulent flows.

In contrast to this test series (e), where the disturbance of the boundary layer started at the outer edge, the disturbance in series (f) originated at the wall. To this end, a continuous square strip (13 by 13 mm) was fitted at a distance of $x = 3m$ from the leading edge of the test plate, crosswise to the direction of flow. The thickness of the boundary layer at this point was about 60 mm. Velocity profiles and wall-shearing stresses were measured at different distances behind the strip. The values for c_f' are reproduced in figure 6a. The test points at shorter distance behind the strip are, of course, lower than for plate flow. With increasing distance, the c_f' values rise steeply to higher values than for plate flow and drop toward the end of the test length, but not as low as for plate flow. The higher c_f' values relative to plate flow are attributable to the increased turbulence caused by the separation at the strip. In figure 6b, the c_f' values, recomputed according to equation (8a), are reproduced. The first point right behind the strip does not fall on the curve of the plate law, while the test points of the order of magnitude of ten boundary-layer thickness already fulfill equation (8) again unequivocally. The reason for the failure of equation (8) for the first test points lies in the fact that the stipulated validity of equation (3) in wall proximity is disturbed by the strip. This fact is borne out by the profiles represented in figure 7 in the manner of figure 1. Profile No. 4 is a profile measured closely behind the strip. A comparison with figure 1 indicates that here in wall proximity, the law, equation (3), is no longer valid. Moreover, the profile is outside of the single-parameter family. Profile No. 1 was measured in the range where equation (8) is applicable again. Note the straight line variation with the same slope as in figure 1 for the validity of equation (3). The plate profile of figure 1 is reproduced for comparison. Figure 7 further shows a profile of the test series with turbulence screen, which again indicates the validity of equation (3) as anticipated from the foregoing.

Figure 8 represents several profiles from the last test series for which equation (8) is applicable again, plotted in the manner of figure 4, along with a plate flow profile for comparison. Here, also, every plotted profile complies with equation (3) in wall proximity.

Translated by J. Vanier
National Advisory Committee
for Aeronautics

REFERENCES

1. Buri, A.: Eine Berechnungsgrundlage für die turbulente Grenzschicht bei beschleunigter und verzögerter Grundströmung. Dissert. Zürich 1931.

2. Gruschwitz, E.: Die turbulente Reibungsschicht in ebener Strömung bei Druckabfall und -anstieg: Ing.-Arch. vol. 2, no. 3, 1931, pp. 321-346.

3. Kehl, A.: Untersuchungen über konvergente und divergente, turbulente Reibungsschichten. Ing.-Arch. vol 13, no. 5, 1943, pp. 293-329.

4. Mangler, W.: Das Verhalten der Wandschubspannung in turbulenten Reibungsschichten mit Druckanstieg. ZWB UM 3052, 1943.

5. Wieghardt, K.: Über die Wandschubspannung in turbulenten Reibungsschichten bei veränderlichem Aussendruck. ZWB UM 6603, 1943.

6. Tillmann, W.: Über die Wandschubspannung turbulenter Reibungsschichten bei Druckanstieg. Diplomarbeit Göttingen 1947.

7. Ludwieg, H.: Ein Gerät zur Messung der Wandschubspannung turbulenter Reibungsschichten. Ing.-Arch. (Available as NACA TM 1284.)

8. Wieghardt, K.: Über einige Untersuchungen an turbulenten Reibungsschichten. ZAMM 25/27, 1947, p. 146.

9. Schultz-Grunow, F.: Neues Reibungswiderstandsgesetz für glatte Platten. Luftfahrtforschung vol. 17, no. 8, 1940, p. 239. (Available as NACA TM 986.)

10. Squire, H. B. and Young, A. D. : The Calculation of the Profile Drag of Aerofoils. R. & M. No. 1838, British A.R.C., 1938.

11. Von Doenhoff, A. E. and Tetervin, N.: Determination of General Relations for the Behaviour of Turbulent Boundary Layers. NACA Rep. 772, 1943.

12. Prandtl, L.: Zur turbulenten Strömung in Rohren und längs Platten. Ergebnisse d. AVA Göttingen, IV. Lieferung, 1932, p. 18.

13. Schoenherr, K. E.: Resistance of Flat Surfaces Moving through a Fluid. Trans. Soc. Naval Architects and Marine Eng. vol. 40, 1932, p. 279.

14. Nikuradse, J.: Turbulente Reibungsschichten an der Platte. ZWB 1942.

15. Falkner, V. M.: A New Law for Calculating Drag. Aircraft Engineering vol. XV, no. 169, 1943, p. 65.

16. Reichardt, H.: Die Wärmeübertragung in turbulenten Reibungsschichten. ZAMM vol. 20, no. 6, 1940, p. 297. (Available as NACA TM 1047.)

17. Wieghardt, K.: Über die Turbulente Strömung im Rohr und längs einer Platte. ZAMM vol. 24, 1944, p. 294.

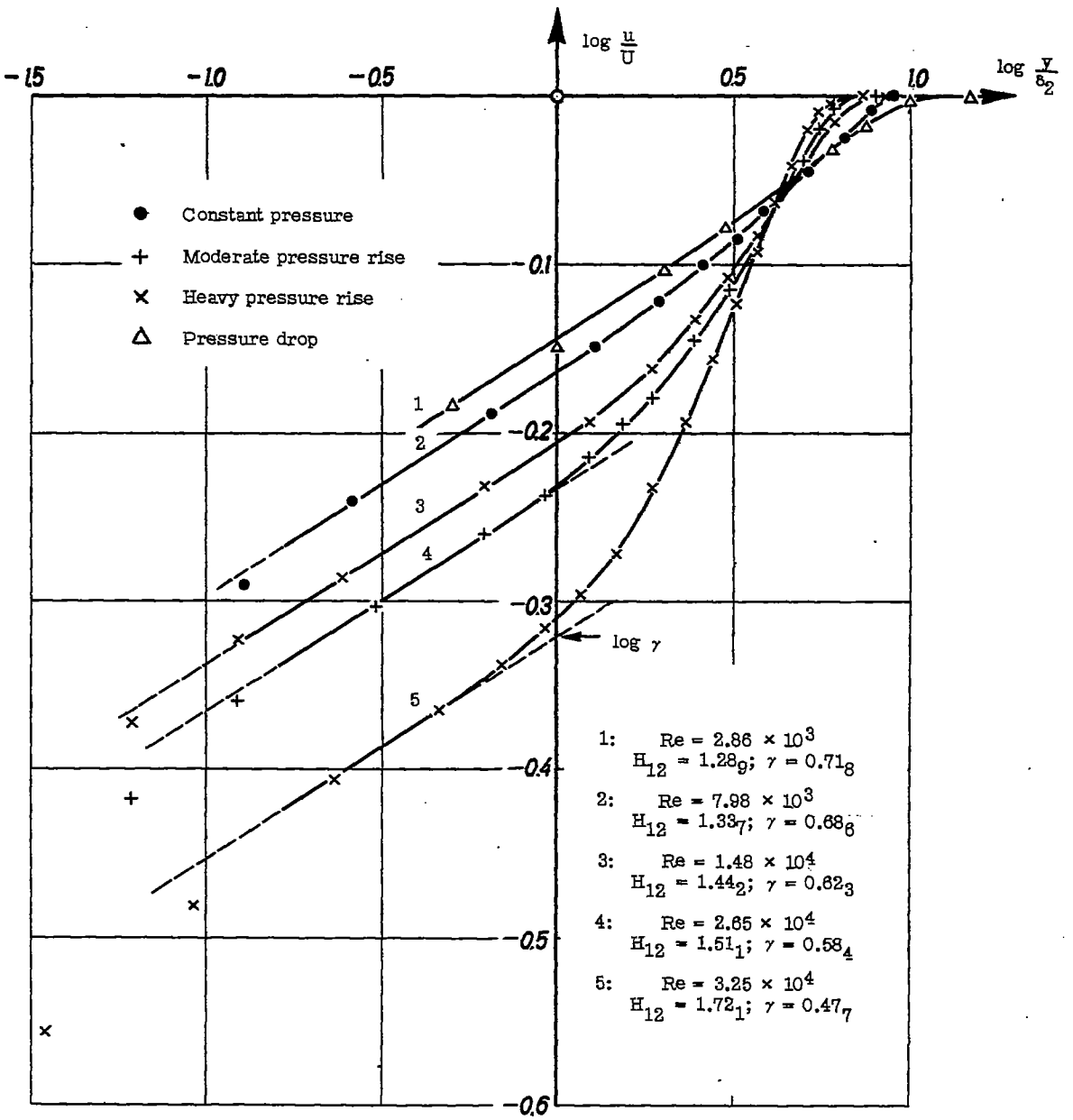

Figure 1.- Single-parametric family of velocity profiles in boundary layers with pressure gradients in dimensionless, double-logarithmic representation.

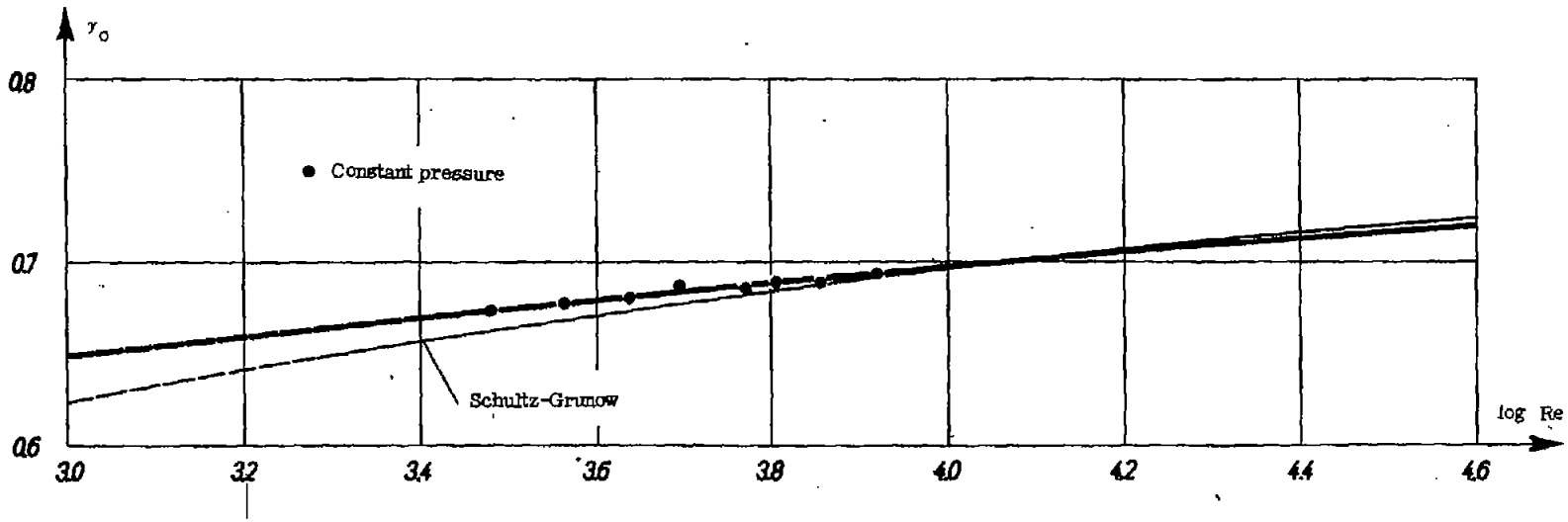

Figure 2.- Profile parameter γ_o of plate flow as function of the Reynolds number Re

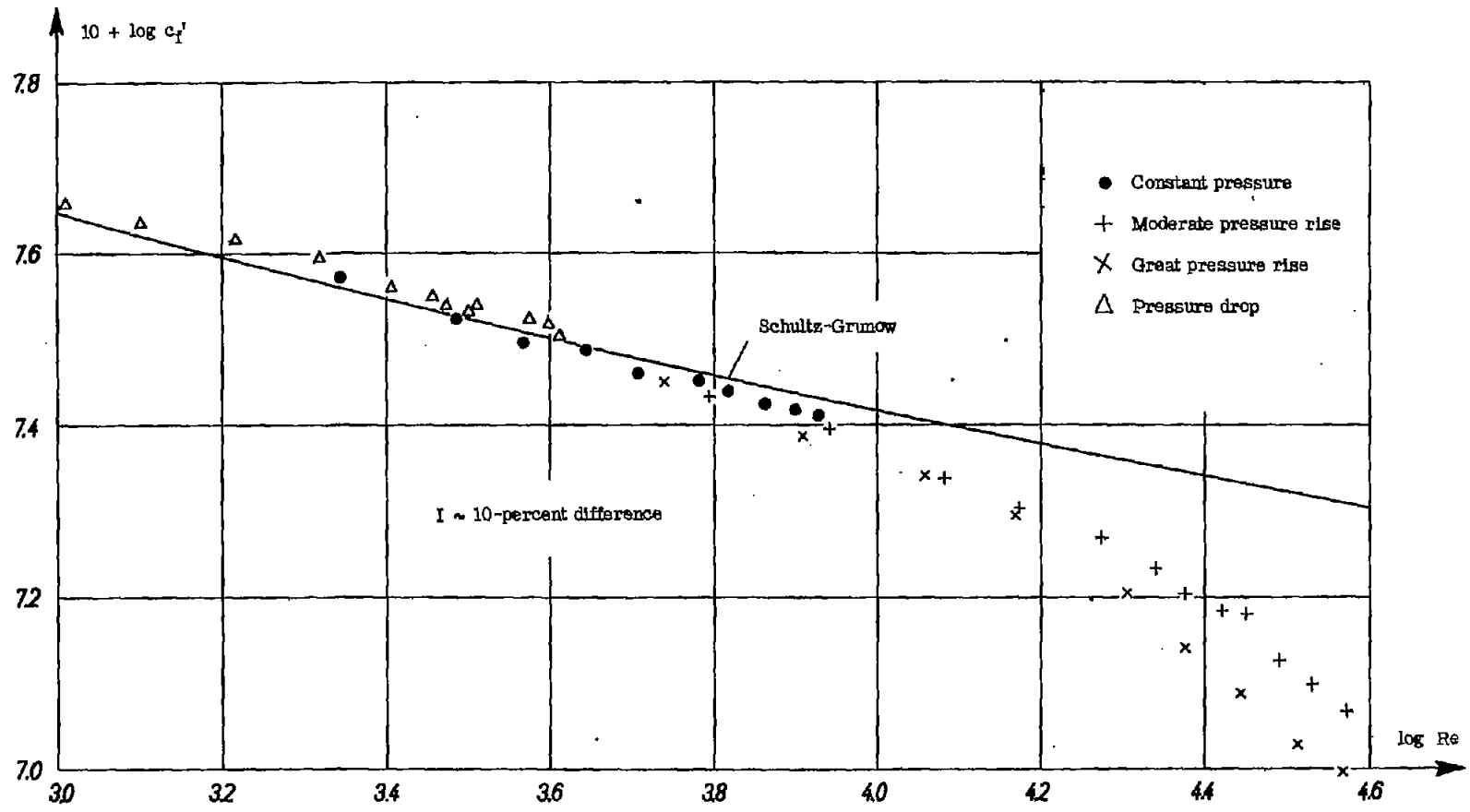

(a) c_f' plotted against Re.

Figure 3.- Drag coefficients c_f' in boundary layers with pressure gradients.

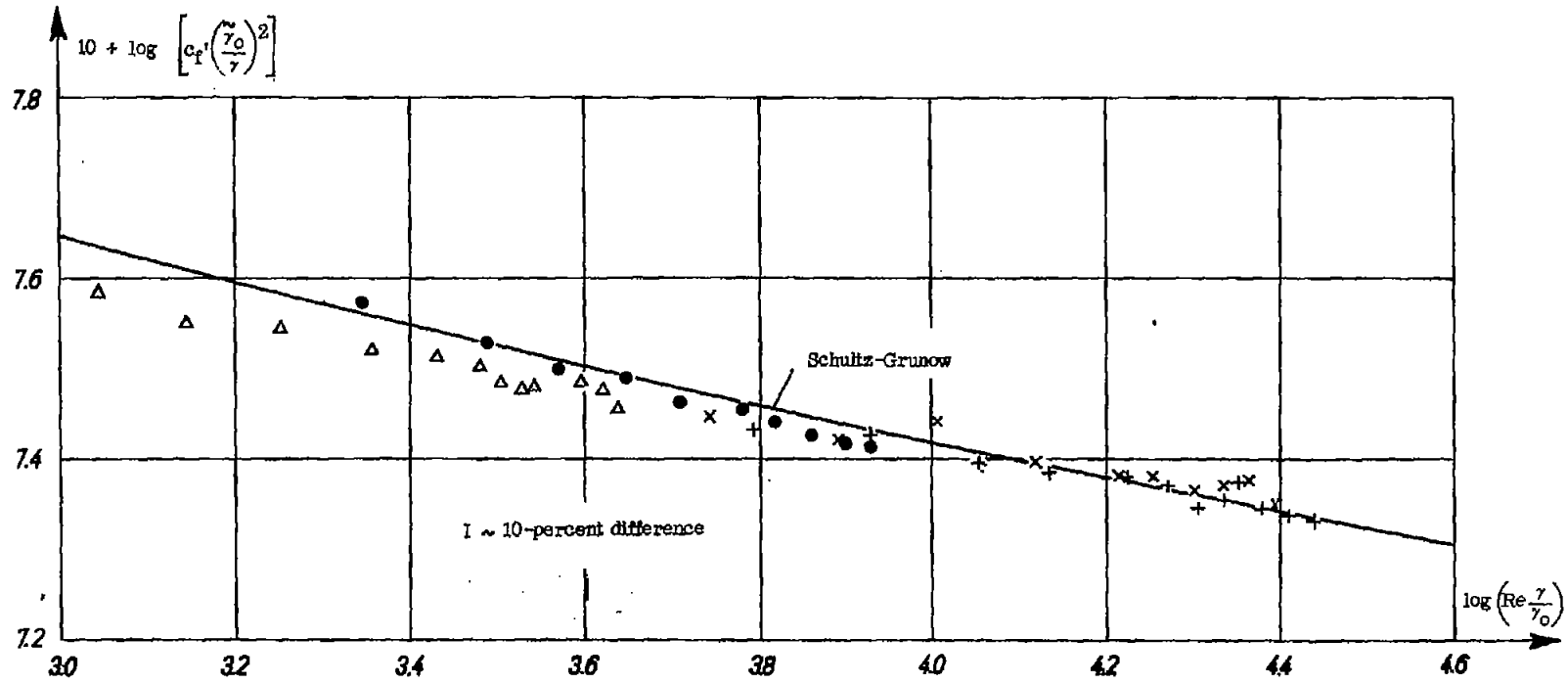

(b) $c_f' \cdot \left(\frac{\gamma_o}{\gamma}\right)^2$ plotted against $\mathrm{Re}\frac{\gamma}{\gamma_o}$ according to equation (8a).

Figure 3.- Concluded.

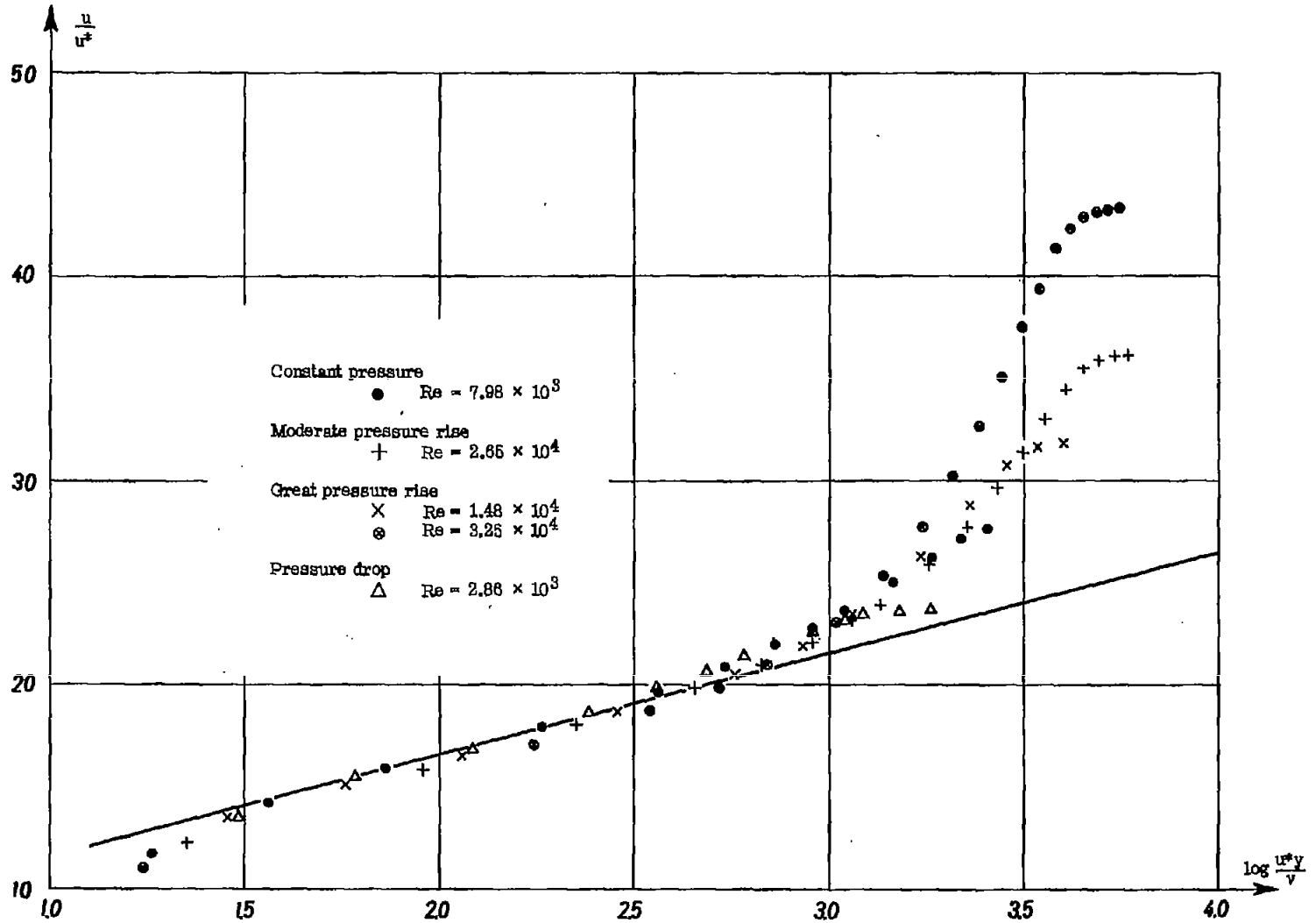

Figure 4.- Several velocity profiles of boundary layers with pressure gradients and universal law, equation (3a), in wall proximity.

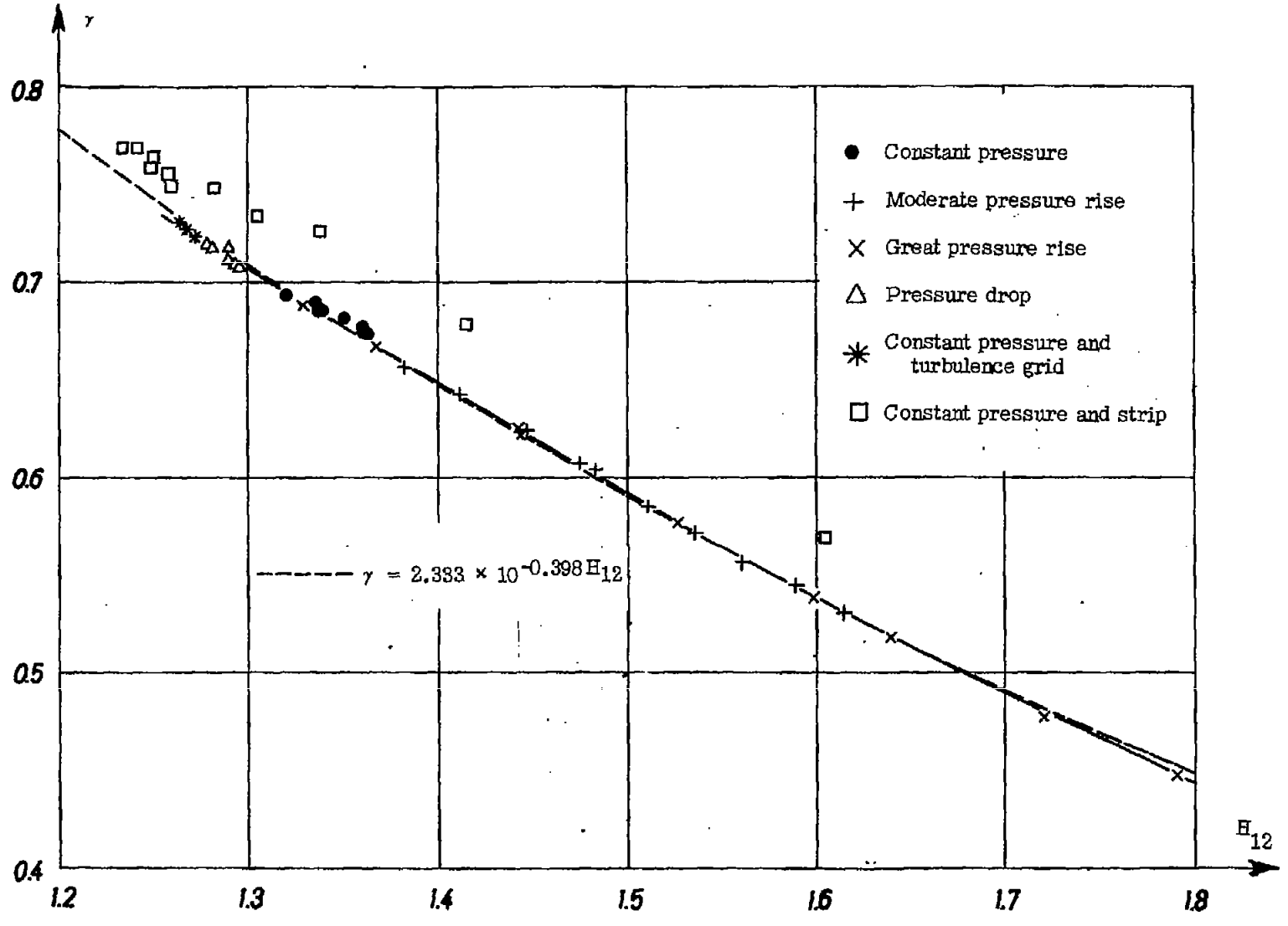

Figure 5.- Relationship between profile parameters γ and H_{12}.

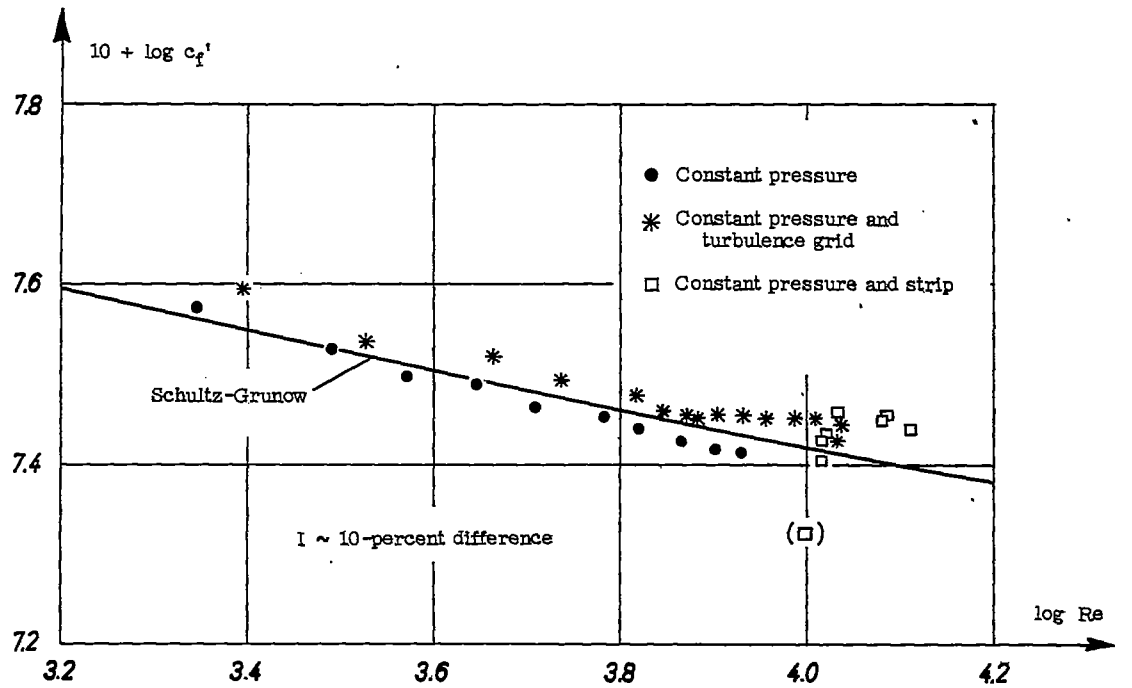

(a) c_f' plotted against Re.

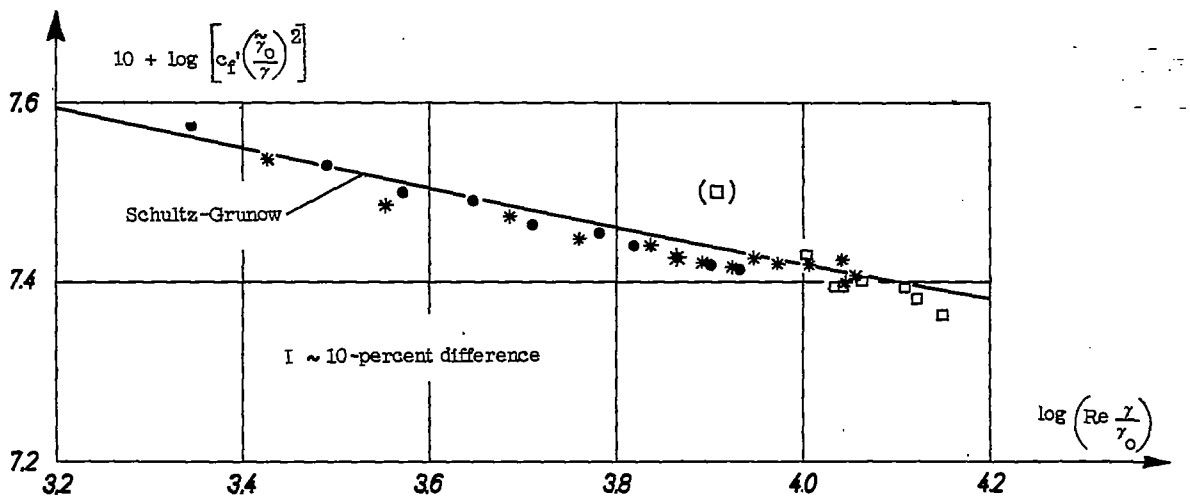

(b) $c_f' \cdot \left(\frac{\tilde{\gamma}_o}{\gamma}\right)^2$ plotted against $\mathrm{Re}\,\frac{\gamma}{\gamma_o}$ according to equation (8a).

Figure 6.- Drag coefficients c_f' in the boundary layers of test series e and f.

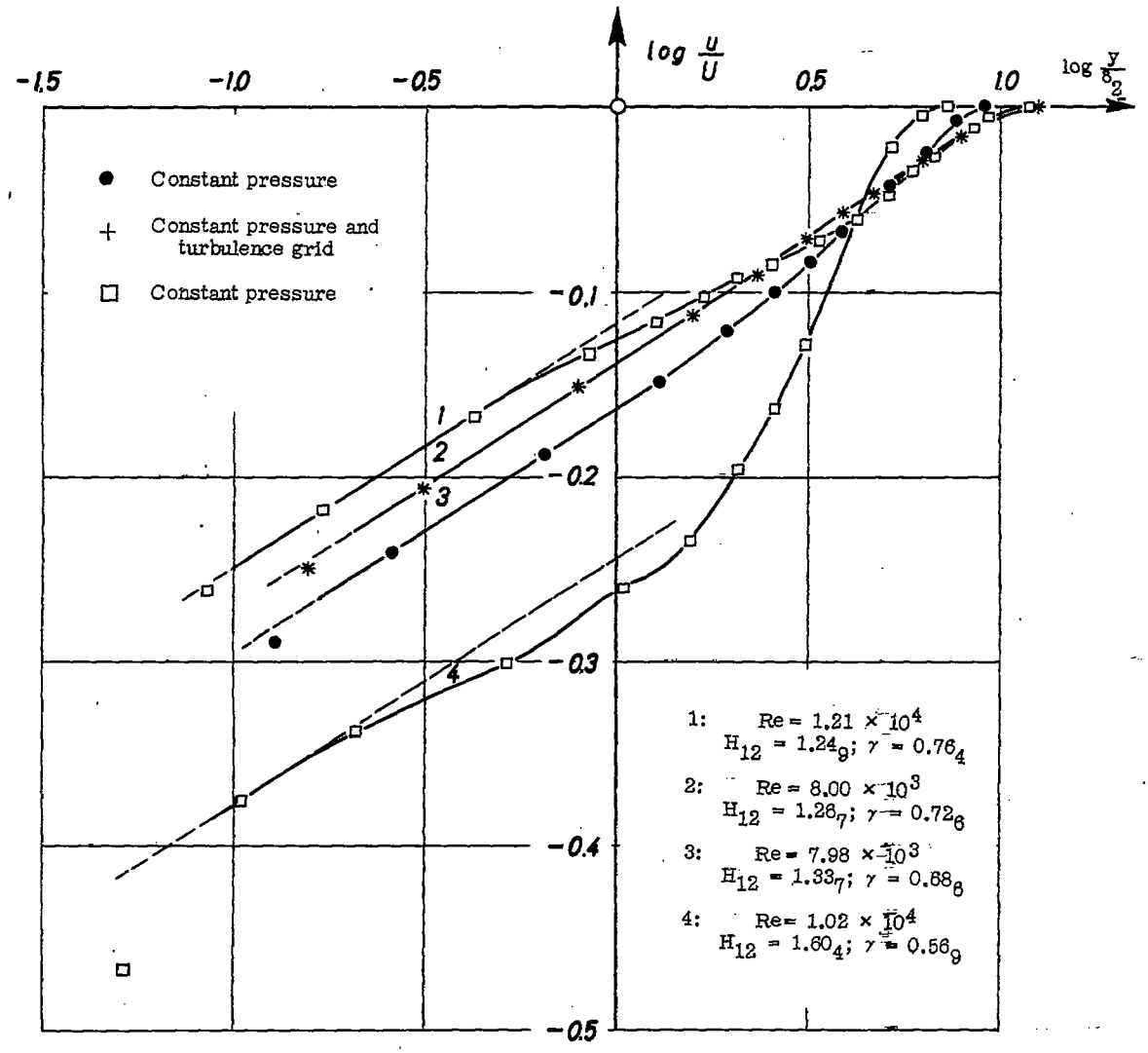

Figure 7.- Several velocity profiles from test series e and f in dimensionless double-logarithmic representation.

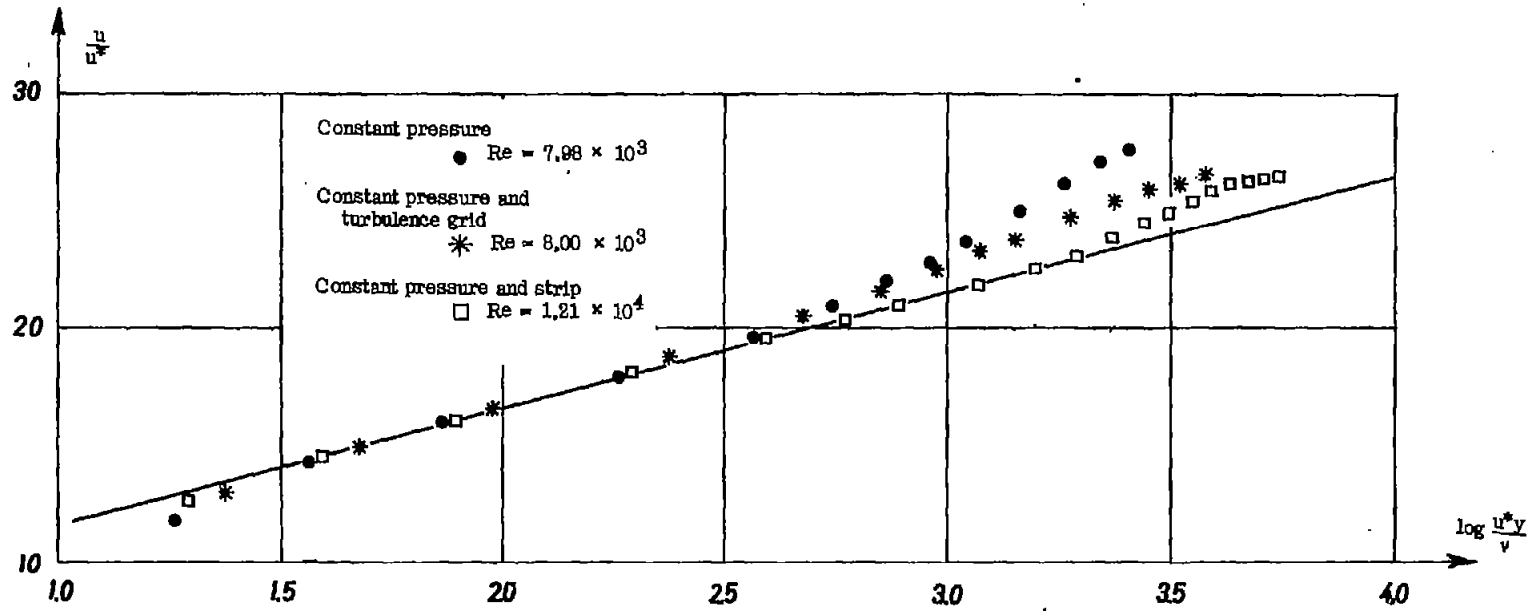

Figure 8.- Several velocity profiles from test series e and f with universal law, equation (3a), in wall proximity.